**Title Page:**

**Afobazole modulates microglial function via activation of both sigma-1 and sigma-2 receptors.**

**Javier Cuevas, Alex Rodriguez, Adam Behensky and Chris Katnik**

JC, AR, AB, CK. Department of Molecular Pharmacology and Physiology, University of South Florida, College of Medicine, 12901 Bruce B. Downs Blvd., MDC-9, Tampa, FL 33612 U.S.A.

**Running Title Page:**


**Running Title:** Sigma receptor modulation of microglia

**Corresponding Author:** Dr. Javier Cuevas; Department of Molecular Pharmacology and

Physiology, University of South Florida College of Medicine, 12901 Bruce B. Downs Blvd.,

MDC-9, Tampa, FL 33612-4799, USA; Voice: (813) 974-4678; Fax: (813) 974-3079; E-mail:

jcuevas@health.usf.edu

**Manuscript information:**

Number of text pages:

Tables: 0

Figures: 11

References: 37

Words in Abstract: 250

Words in Introduction: 592

Words in Discussion: 1409

**Abbreviations:** Afob, afobazole; AM, acetoxymethyl ester; ASIC, acid-sensing ion channels;

BD 1063, 1-[2-(3,4-dichlorophenyl)ethyl]-4-methylpiperazine dihydrochloride; ; BD 1047, N-[2-

(3,4-Dichlorophenyl)ethyl]-N-methyl-2-(dimethylamino)ethylamine dihydrobromide; DMSO,

dimethyl sulfoxide; DTG, 1,3-di-*o*-tolyl-guanidine; HEPES, N-(2-Hydroxyethyl)piperazine-N'-2-

ethanesulfonic Acid; MET, metaphit; PBS, phosphate buffered saline; PSS, physiological saline

solution; $[Ca^{2+}]_i$, intracellular calcium concentration; $\Delta[Ca^{2+}]_i$, change in intracellular calcium

concentration; LDH, lactate dehydrogenase; TNF-$\alpha$, tissue necrosis factor-alpha.


**Recommended Section Assignment:** Neuropharmacology

**Abstract:**

Microglial cells play a critical role in the neuroinflammatory response that accompanies various diseases of the central nervous system, such as ischemic stroke, and ATP is a major signaling molecule regulating the response of these cells to these pathophysiological conditions. Experiments were carried out to determine the effects of afobazole on microglial function and to identify the molecular mechanisms by which afobazole affects microglial cells. Afobazole was found to inhibit migration of microglial cells in response to ATP and UTP chemoattraction in a concentration dependent manner. Inhibition of either σ-1 or σ-2 receptors decreased the effects of afobazole on microglia. In addition to inhibiting microglial cell migration, activation of σ receptors by afobazole decreased intracellular calcium elevation produced by focal application of ATP and UTP in isolated microglial cells. Furthermore, afobazole blocked membrane currents elicited by rapid application of ATP in microglial cells. Taken together, our data indicate that afobazole inhibits microglial response to P2Y and P2X purinergic receptor activation by functioning as a pan-selective σ receptor agonist. In addition to modulating response to purinergic receptor activation, the effects of afobazole on microglial survival during in vitro ischemia were assessed. Application of afobazole during in vitro ischemia decreased microglial cell death during the ischemic episode and after a 24 hr recovery period. Moreover, when afobazole was only applied following the ischemic episode, a significant enhancement in cell survival was still observed. Thus, afobazole acts via σ receptors to decrease microglial response to ATP and provides cytoprotection during and after ischemia.

**Introduction:**

Microglia are the resident macrophages of the brain, and constitute nearly 10% of the total cell population of this organ. The function of these cells in normal and pathophysiological conditions has been an area of significant research, and considerable controversy surrounds the role of these cells in diseases of the CNS. It has been shown that microglia transform from a resting state to an activated state in response to various stimuli, such as neuronal injury or pathogen infiltration (Hanisch and Kettenmann, 2007). Upon stimulation, these cells migrate to the site of injury, phagocytose debris and release proinflammatory compounds (Hanisch and Kettenmann, 2007). Such a microglial response has been reported to occur as a result of an ischemic insult to the brain, following which microglia are attracted to the site of injury and proliferate (Weinstein et al., 2010). It has been suggested that these microglia then contribute to the neuroinflammatory response that results in the demise of neurons (Rogove et al., 2002; Streit et al., 2004; Dheen et al., 2007). Thus, there is significant interest in finding agents that modulate the function of microglia and reduce their proinflammatory response.

Microglial cells are highly susceptible to ischemic injury and are more likely to undergo apoptosis than astrocytes following an ischemic insult (Lyons and Kettenmann, 1998). In contrast to the theory that microglia compound neuronal injury following stroke, it has been suggested that non-activated microglia can provide neurotrophic factors that lessen the inflammatory response and can mitigate neuronal death (Lalancette-Hebert et al., 2007). It has also been shown that injection of microglia into the lateral ventricles of adult rats undergoing a middle cerebral artery occlusion results in migration of the transplanted cells into the infarcted striatum and reduction of infarct size (Kitamura et al., 2004). Thus, enhancing the survival of microglia may be of significant benefit following stoke injury.

Studies in our laboratory have shown that sigma receptors in microglial cells can significantly decrease the conversion of these cells into the activated state and depress production of proinflammatory mediators (Hall et al., 2009). This suppression of microglial

activation may in part explain why the sigma receptor agonist, DTG, can decrease neuronal injury in a rat model of ischemic stroke even when administered at delayed time points (Ajmo et al., 2006). However, the specific sigma receptor involved in these effects has not been identified. Furthermore, how sigma receptor activation influences microglial survival following ischemia remains to be determined.

Afobazole (5-ethoxy-2-[2-(morpholino)-ethylthio]benzimidazole), an anxiolytic currently in clinical use in Russia, has shown potential both in vitro and in vivo as a neuroprotective agent (Galaeva et al., 2005; Zenina et al., 2005; Seredenin et al., 2008). To date, however, the effects of afobazole on microglial cell function and survival has not been studied. Given that afobazole may act as a sigma receptor ligand, it is of significant interest to determine how afobazole affects microglial responses and if the effects of this drug are linked to the activation of sigma receptors.

Experiments were carried out to examine the effects of afobazole on several key markers of microglial activation and to determine the molecular mechanisms and pathway(s) underlying these effects. Afobazole was found to inhibit microglial migration in response to ATP and UTP. These effects of afobazole were due to activation of both σ-1 and σ-2 receptors. Afobazole acting via both σ receptor subtypes decreased P2Y- and P2X- mediated responses, resulting in decreases in $[Ca^{2+}]_i$ elevations and membrane currents produced by the purinergic receptors. Moreover, afobazole enhanced microglial survival following ischemia, even when the drug was applied only after the ischemic insult.

**Methods:**

*Primary Cultures of Microglia*

Primary cultures of microglia were prepared from Sprague-Dawley rat pups (post natal day 3-4) as previously described by our laboratory (Hall et al., 2009). The mixed glial cultures were incubated for 7-12 days at 37 $^\circ$C prior to experiments being carried out. Microglia were separated from other cells, physically, by shaking the flasks containing the mixed cultures at high speed. Following shaking, the supernatant was collected and spun at 2200 rpm. The cell pellet was resuspended in DMEM. Cells were used immediately for the migration and cytotoxicity assays or plated on poly-L-lysine coated glass coverslips for one day prior to use in calcium imaging or electrophysiological experiments.

*Migration Assay*

Migration assays were carried out using a 48-well microchemotaxis chamber (Neuro Probe, Inc., Gaithersburg, MD). The bottom wells of the chamber were filled with the chemoattractant (ATP or UTP) in DMEM in the absence and presence of chemicals tested (i.e. afobazole ± σ ligands). The upper chamber contained $1 \times 10^6$ freshly isolated microglia suspended in DMEM, also with or without afobazole ± σ ligands to match the chemical milieu of the lower chamber. The two chambers were separated by a polycarbonate membrane containing 8 μm pores at a density of $1 \times 10^3$ pores/mm$^2$ (exposed filter area was 8 mm$^2$). Prior to experiments, the membrane was coated with fibronectin at 10 μg/ml in phosphate buffer saline solution (PBS) containing (in mM): 144 NaCl, 10 Na$_2$HPO$_4$, 3 KH$_2$PO$_4$ (pH to 7.4 with NaOH) for 1hr at room temperature. The microglia were permitted to migrate for 2 hr while incubated at 37$^\circ$C. The membranes were then removed and non-migrating microglia adhering to the top of the membrane were scraped off. The membrane was then incubated in 4 %

6

paraformaldehyde in PBS for 15 minutes at room temperature, washed 2 times in ice cold PBS, and washed once in distilled water. The membrane was then cut to separate the wells and placed on microscope slides, membrane bottom facing up. Once the membrane had dried, Vectashield Hardset mounting media containing 4'-6-Diamidino-2-phenylindole (DAPI) (Vector Labs, Burlingame Ca) was applied to the membrane and a coverslip affixed to the slide. Cells were illuminated at 359 nm and visualized at 461 nm using a Zeiss Axioskop 2 outfitted with a 20X objective. Images were collected using OPENLAB software (PerkinElmer, Walthham, MA) and analyzed using ImageJ (NIH). Stained nuclei were isolated from the fainter visible pores by setting excluding size (30-300 $\mu m^2$) and intensity thresholds. DAPI positive cells were identified and counted in 4 random fields/well. The number of cells which migrated in each well was taken as the average number of cells in the 4 fields of view. For each experiment, a minimum of three wells were used, and the results of at least three experiments were averaged together.

*Calcium imaging measurements*

The effects of afobazole on intracellular $Ca^{2+}$ elevations produced by ATP and UTP were examined using fluorescent imaging techniques with fura-2 as the indicator as previously reported (Hall et al., 2009). Microglia plated on coverslips were incubated for 1 hour at room temperature in DMEM containing 3 $\mu$M acetoxymethyl ester fura-2 and 0.3 % dimethyl sulfoxide. The coverslips were washed in fura-2-free saline solution prior to the experiments. The control bath solution for calcium imaging and electrophysiological experiments was a physiological saline solution (PSS) containing (in mM): 140 NaCl, 5.4 KCl, 1.3 $CaCl_2$, 1.0 $MgCl_2$, 20 glucose, and 25 HEPES (pH to 7.4 with NaOH). All drugs for the calcium imaging and electrophysiological studies were applied in PSS using a rapid application system as described previously (Cuevas and Berg, 1998).

7

*Electrophysiology recordings*

Microglia plated on glass coverslips were moved to a recording chamber mounted on a Zeiss Axiovert 200 and visualized at 400x. Methods for the electrical recordings of these cells were identical to those used previously in our laboratory to record from neurons (Herrera et al., 2008). Cells were electrically accessed using the amphotericin B perforated-patch method (Rae et al., 1991). An amphotericin B stock solution (60 mg/ml in DMSO) was made daily, kept on ice, light protected, and diluted to 240 µg/ml (0.4% DMSO) in control pipette solution immediately prior to patch clamp experiments. The pipette solution consisted of (in mM): 75 $K_2SO_4$, 55 KCl, 5 $MgSO_4$, and 10 HEPES (titrated to pH 7.2 with N-methyl-d-glucamine). Patch electrodes were made from thin-walled borosilicate glass (World Precision Instruments Inc., Sarasota, FL) and had resistances of 1.0–1.5 MΩ. Only cells with stable access resistance ($R_s$) ≤ 20 MΩ throughout experiment were used, and this resistance was always compensated at 40%. All cells were voltage-clamped at -70 mV.

*Reagents*

All chemicals used in this investigation were of analytic grade. The following drugs were used: amphotericin B, DTG and metaphit (1-(1-(3-Isothiocyanato)phenyl)cyclohexylpiperidine) (Sigma-Aldrich, St. Louis, MO), SM-21 ((±)-Tropanyl 2-(4-chlorophenoxy)butanoate maleate), rimcazole (9-[3-(cis-3,5-Dimethyl-1-piperazinyl)propyl]-9H-carbazole dihydrochloride), NE-100 (4-Methoxy-3-(2-phenylethoxy)-N,N-dipropylbenzeneethanamine hydrochloride), BD 1063 (1-[2-(3,4-dichlorophenyl)ethyl]-4-methylpiperazine dihydrochloride) and BD 1047 (N-[2-(3,4-Dichlorophenyl)ethyl]-N-methyl-2-(dimethylamino)ethylamine dihydrobromide) (Tocris Bioscience, Ellisville, MO), and fura-2 acetoxymethyl ester (Molecular Probes, Eugene, OR). Afobazole was generously provided by Masterclone.

_Data analysis_

Data analysis of $Ca^{2+}$ imaging and electrophysiological studies were carried out using Clampfit 9 (Axon instruments).  Imaging data files were collected using SlideBook 4.02 (Intelligent Imaging Innovations, Inc.), converted to text format and imported into Clampfit for final analysis. Statistical analysis was conducted using SigmaPlot 9 and SigmaStat 3 software (Systat Software, Inc.).  For migration results, n value refers to runs, with 3 wells per run for each condition. Statistical differences were considered significant if $p < 0.05$.  Differences were determined using paired and unpaired t-tests for within group and between group experiments, respectively.  Similarly, either a 1-way or a 2-way ANOVA (with or without repeat measures) was used for multiple group comparisons, as appropriate.  Post-hoc analysis of the ANOVA data was conducted when necessary using a Tukey's Test to determine differences between individual groups.  For the generation of concentration response curves, data were best fit using a single-site or two-site Langmuir-Hill equation.

**Results:**

The release of ATP from injured or dying neurons is one of the earliest signals involved in the activation of microglia following brain injury (Davalos et al., 2005). ATP, acting via ionotropic (P2X) and metabotropic (P2Y) purinergic receptors on microglia, causes these cells to migrate to the site of injury (Honda et al., 2001). Thus, experiments were carried out to determine how afobazole affects the migration of microglial cells in response to ATP, which activates both P2X and P2Y receptors, and UTP, which selectively activates P2Y receptors. Figure 1A shows photomicrographs of microglial nuclei stained using DAPI. The bright, visible nuclei represent microglial cells that have migrated across a polycarbonate filter in a chemotaxis chamber over a two hour period in response to 100 $\mu$M ATP (left panels) or 100 $\mu$M UTP (right panels) in the absence (Control) and presence of afobazole at the indicated concentrations. Application of afobazole decreased the number of migrating microglia. This decrease in the number of cells was not due to changes in survival rates of the cells (data not shown). In identical experiments, afobazole produced a concentration-dependent decrease in microglial migration. Figure 1B shows the concentration response relationship for afobazole inhibition of microglial migration in response to ATP and UTP. For both compounds, the concentration-response relationship was best fit by a two-site Langmuir-Hill equation.

Activation of sigma receptors has been linked to inhibition of microglial cell migration and afobazole has been suggested to interact with sigma receptors (Seredenin et al., 2009). Experiments were carried out to determine if afobazole acts through $\sigma$ receptors in microglial cells to inhibit migration. Preincubation of microglial cells in the pan-selective, irreversible $\sigma$ receptor antagonist, metaphit, decreased the migration of microglia (Figure 2A). However, a similar number of cells migrated in the presence of afobazole with and without metaphit preincubation (Figure 2A). Thus, metaphit had effects on microglial migration on its own, but

10

effectively disrupted afobazole inhibition of migration. The inhibition of migration observed under control conditions (no metaphit preincubation, Media) was 46 ± 2%, but decreased to 27 ± 2 following metaphit preincubation (Figure 2B). Similar results were observed when the pan-selective σ receptor agonist, DTG, was used (Figures 2A & 2B). When UTP was used as the chemoattractant, metaphit once again decreased migration on its own (Figure 2C). However, the number of migrating cells was greater when afobazole was applied following metaphit preincubation than when afobazole was applied alone (Figure 2C). The net result is a decrease in afobazole-induced inhibition of migration from 49 ± 1% (Media) to 25 ± 1% when cells were preincubated in metaphit (Figure 2D). As with ATP, DTG inhibited UTP-evoked migration in a metaphit-sensitive manner (Figures 2C and 2D)

To date, the specific σ receptor subtype(s) responsible for inhibiting microglial migration has not been identified. Thus, σ receptor subtype-selective antagonists were used to determine the specific σ receptor subtype responsible for the afobazole-evoked inhibition of microglial cell migration. Figure 3A shows the mean number of cells migrating (per field of view) when ATP was applied alone (ATP) or along with three different σ-1 receptor selective antagonists (BD 1063, BD 1047 and NE-100). Afobazole was then applied along with the ATP (Afob) or with the ATP and the σ-1 antagonists (Afob + BD 1063, Afob + BD 1047 and Afob + NE-100). Like metaphit, all σ-1 receptor antagonists produced a small inhibition of migration on their own (Figure 3A). However, a greater number of microglial cells migrated in the presence of afobazole when these σ-1 antagonists were applied than when afobazole was administered alone (Figure 3A). The net result was that afobazole-mediated inhibition of ATP-evoked migration was decreased by ≥ 47% when the σ-1 receptor antagonists were co-applied (Figure 3B). Thus, inhibition of σ-1 receptors decreases afobazole-evoked inhibition of microglial migration.

To determine if σ-2 receptors are also involved in the regulation of microglial cell migration by afobazole, σ-2 receptor selective antagonists were used in a series of experiments. Like σ-1 antagonists and metaphit, σ-2 selective antagonists produced a small decrease in microglial cell migration when applied alone (Figure 4A). However, when applied with afobazole, both SM-21 and rimcazole significantly lessened the inhibition of migration produced by afobazole (Figure 4AB). There was a 44 ± 0.3% decrease in migration in the afobazole-treated group, but only a 22 ± 0.5% and a 31 ± 0.4% decrease when afobazole was applied along with SM-21 and rimcazole, respectively (Figure 4B).

Given the link between σ receptors, intracellular calcium and ATP-evoked microglial cell migration, experiments were carried out to determine if afobazole can suppress elevations in $[Ca^{2+}]_i$ evoked by ATP. Figure 5A shows representative traces of $[Ca^{2+}]_i$ as a function of time recorded from two cells exposed to ATP in the absence (Control) and presence of 100 μM afobazole (Afobazole, upper traces) and 100 μM DTG (DTG, lower traces). Both afobazole and DTG reduced ATP-evoked increases in $[Ca^{2+}]_i$. In identical experiments, both peak (Figure 5B, left panel) and net $[Ca^{2+}]_i$ elevations (Figure 5B, right panel) were decreased by afobazole and DTG. Afobazole and DTG decreased peak $[Ca^{2+}]_i$ elevations produced by 100 μM ATP by 81 ± 2% and 58 ± 4%, respectively.

Microglia express both metabotropic (P2Y) and ionotropic (P2X) purinergic receptors and both of these receptors can contribute to increases in $[Ca^{2+}]_i$. To determine if σ receptors can regulate ionotropic receptors, whole-cell patch-clamp electrophysiological recordings were carried out. Figure 6A shows traces of membrane currents recorded from a single microglia held at -70 mV in response to focal application of 300 μM ATP. ATP evoked a rapidly activating inward current that decayed over time. Application of 300 μM afobazole decreased the peak response elicited by ATP (Figure 6A). Compiling the data from similar experiments

demonstrates that 300 μm afobazole significantly decreases ATP-evoked currents by approximately 50%. Thus, afobazole can affect P2X channels.

The relationship between afobazole interaction with σ receptors and regulation of ATP-evoked $[Ca^{2+}]_i$ elevations in microglia was examined pharmacologically. The pan-selective σ receptor antagonist, metaphit, was used to inhibit σ receptor function in microglia and the effects of afobazole on ATP-evoked $[Ca^{2+}]_i$ elevations studied using $Ca^{2+}$ fluorometry. Figure 7A shows $[Ca^{2+}]_i$ traces as a function of time recorded from two isolated microglial cells. Both cells were stimulated with 100 μM ATP in the absence and presence of 100 μM afobazole, but the traces on the right are from a cell preincubated in metaphit. While afobazole decrease the $[Ca^{2+}]_i$ responses in both cells, afobazole was more effective in the cell preincubated in PSS alone. A comparison of results obtained from multiple cells shows that afobazole significantly decreases ATP-evoked $[Ca^{2+}]_i$ increases in the absence and presence of metaphit preincubation, but that metaphit preincubation diminishes the effects of afobazole (Figure 7B). Afobazole (100 μM) inhibition of the ATP-evoked rise in $[Ca^{2+}]_i$ decreases from 48 ± 4% to 21 ± 3% following metaphit preincubation (Figure 7C).

While afobazole inhibition of P2X channels may account for the decrease in $[Ca^{2+}]_i$, the effects of afobazole on P2Y-mediated $[Ca^{2+}]_i$ responses remains to be studied. Application of the P2Y agonist, UTP (100 μM), evoked increases in $[Ca^{2+}]_i$ similar to those elicited by ATP (Figure 7D). In two individual microglia, afobazole (100 μM) decreased $[Ca^{2+}]_i$ responses to UTP, but the response to afobazole was reduced by preincubation in metaphit (Figure 7D). In identical experiments, it was found that preincubation in metaphit produced a small but significant reduction in the UTP-evoked elevation in $[Ca^{2+}]_i$ (Figure 7E). Interestingly, the $[Ca^{2+}]_i$ response observed when afobazole was applied following metaphit preincubation was greater than that observed in control cells (PSS, Figure 7E), indicating that the effects of afobazole were diminished by metaphit preincubation. The inhibition UPT-evoked increases in $[Ca^{2+}]_i$ by

afobazole decreased from 59 ± 4% in the absence of metaphit preincubation (PSS) to 25 ± 2% in the presence of metaphit preincubation (Figure 7F).

Experiments using the σ-1 receptor selective antagonists, BD 1063 and BD 1047, were carried out to ascertain if that σ receptor subtype is specifically involved in the effects of afobazole on ATP- and UTP-evoked increases in microglial $[Ca^{2+}]_i$. Neither BD 1063 (100 $\mu$M) nor BD 1047 (10 $\mu$M) significantly affected ATP-evoked increases in $[Ca^{2+}]_i$ (Figures 8A & 8B). However, in the presence of these σ-1 receptor antagonists the effects of afobazole (100 $\mu$M) on the $[Ca^{2+}]_i$ responses to ATP were significantly decreased (Figures 8A & 8B). Both BD 1063 (100 $\mu$M) and BD 1047 (10 $\mu$M) reduced the percent inhibition produced by afobazole by approximately 30% (Figures 8C & 8D).

Given that σ-2 receptors are also involved in afobazole modulation of microglial migration, the role of these receptors in afobazole regulation of ATP-evoked increases in $[Ca^{2+}]_i$ was also tested. The σ-2 receptor selective antagonists SM-21 and rimcazole were used in an attempt to disrupt afobazole signaling via this receptor. Figure 9 shows the results obtained in these experiments. Application of either SM-21 or rimcazole blunted the inhibitory effects of afobazole on mean peak ATP-evoked $[Ca^{2+}]_i$ elevations (Figures 9A & 9B). There was an approximately 30% reduction in the afobazole-induced percent inhibition of the $[Ca^{2+}]_i$ responses in the microglial cells when either of these σ-2 antagonists were applied (Figures 9C & 9D).

Studies have shown that microglia are highly susceptible to ischemic injury (Lyons and Kettenmann, 1998) and numerous studies have suggested that these cells are important for limiting injury following ischemic stroke (Weinstein et al., 2010). Thus, experiments were carried out to determine if afobazole can provide cytoprotection in vitro during ischemia. Cultured microglia were exposed to a combination of oxygen-glucose deprivation and 4 mM azide for 2 hours in order to stimulate ischemia-induced cell death. Microglial cell death was quantified

14

using an LDH cytotoxicity assay. Figure 10A shows the relative degree of cell death observed under control conditions (Control, normoxia and normal media) and when microglial cells were exposed to the ischemic conditions (Ischemia). Under both conditions, cells were treated with either no drug (DMEM) or with DTG and afobazole at the indicated concentrations (in μM). Both afobazole and DTG significantly decreased neuronal death immediately following ischemia in a concentration-dependent manner. When microglial cells were removed from the ischemic environment and placed in normal media during a 24 hr recovery period, cell death continued at a faster rate in cells exposed to ischemia than in control cells (Figure 10B). Both afobazole and DTG decreased the amount of microglial cell death that occurred after this 24 hr recovery (Figure 10B). Combining the data for cell death during the ischemic episode and during the recovery period shows that microglial cell death during ischemia is nearly 3-fold that of control and that both afobazole and DTG enhance cell survival (Figure 10C). Moreover, afobazole at 100 μM was more cytoprotective than DTG at that same concentration (Figure 10C). Specifically examining the ischemia-induced cell death shows that afobazole and DTG decrease cell death following the ischemic episode in a concentration-dependent manner, and both inhibit this cell death by approximately 40% (Figure 10D). The ischemia-induced cell death that occurs during the 24 hr recovery period was likewise reduced by these drugs, but the effects ranged from 64 ± 3% (30 μM DTG) to 78 ± 4% (100 μM afobazole) (Figure 10E). The effect of these drugs on net microglial cell death was concentration and drug dependent (Figure 10F). The most pronounced cytoprotection observed was provided by 100 μM afobazole, which reduced net cell death by over 50% (Figure 10F).

There is significant interest in identifying agents that can provide neuroprotection and cytoprotection after an ischemic event has occurred. Thus, experiments were conducted to determine if application of afobazole after in vitro ischemia can affect microglial survival. Figure 11A shows the result of multiple experiments in which microglial cells were exposed to ischemia

15

for 2 hrs and later treated with either media (DMEM) as a control or with afobazole at 30 μM and 100 μM concentrations.  As expected, there was no difference in the cell death observed for all three groups during the ischemic event, since all groups were treated with DMEM at this stage (Figure 11A).  Introduction of afobazole after the ischemic event (DMEM-Afob 30, DMEM-Afob 100), decreased the cell death that occurs during a 24 hr recovery period after the ischemic episode (Figure 11B).  The reduction in microglial cell death observed with this delayed application of afobazole (DMEM-Afob 30, DMEM-Afob 100) was comparable to that seen when afobazole was applied both during the ischemic event (Figure 11B, compare with Figure 10B).  When net cell death (during ischemia + recovery) is compared for these groups, delayed application of afobazole produced a statistically significant reduction in cell death (Figure 11C).  However, administration of afobazole throughout was the most effective treatment paradigm for reducing cell death (Figure 11C).  Looking specifically at the ischemia-evoked component of cell death, there was no protection in the DMEM followed by afobazole groups, as expected (Figure 11D).  Delayed application of afobazole, however, decreased ischemia-induced microglial cell death by > 60% (Figure 11E).  Figure 11F shows the percent inhibition of net ischemia-evoked cell death.  Delayed application of afobazole was able to reduce microglial cell death by approximately 20% at both concentrations tested (Figure 11F).

**Discussion:**

The major discovery reported here is that afobazole acts through both σ-1 and σ-2 receptors to influence activation and survival in microglial cells. To the best of our knowledge, this is the first report of afobazole affecting the function of glial cells. Migration of microglial cells in response to ATP and UTP were blocked by afobazole, and this inhibition could be disrupted via the use of pan-selective (metaphit) and subtype selective (σ-1, NE-100, BD 1063 and BD 1047; σ-2, SM-21 and rimcazole) σ receptor antagonists. In addition to disrupting microglial migration, afobazole blocked membrane currents evoked by ATP and calcium elevations elicited by ATP and UTP. The effects on $Ca^{2+}$ increases could be blocked via the use of σ receptor antagonists, indicating that afobazole acting on σ-1 and σ-2 receptors can decrease P2X and P2Y receptor function. Finally, data presented here show that afobazole can also protect microglial cells from ischemic injury, and application of this drug, even at delayed time points, can enhance survival of these cells in an in vitro ischemia model.

Previous studies in our laboratory had shown that stimulation of σ receptors can decrease microglial cell activation in response to various stimuli, including ATP, MCP-1 and lipopolysaccharide (Hall et al., 2009). However, the specific σ receptor involved remained to be identified. Furthermore, the possibility that afobazole could act as an agonist at one or both of these receptors to influence microglial activation remained unexplored. We show here that application of afobazole can completely abolish the migration of microglia in response to both ATP and UTP. The effects of afobazole were blocked by preincubating the cells in the pan-selective, irreversible inhibitor of σ receptors, metaphit. The concentration required and extent of the block are consistent with the effects of afobazole being mediated by actions of this drug on σ receptors (Zhang and Cuevas, 2002; Wu, 2003; Katnik et al., 2006; Herrera et al., 2008).

The role of σ receptors in the actions of afobazole on migration were further supported via the use of subtype-selective antagonists. Three σ-1 receptor-selective antagonists, NE-100, BD

17

1063 and BD 1047, decreased the ability of afobazole to inhibit microglial migration. At the same concentration used here (100 μM), NE-100 has been shown to block σ-1 receptor-mediated protection against oxidative stress in human retinal cells (Bucolo et al., 2006). BD 1063 and BD 1047 were first shown to be effective inhibitors of σ-1 receptors by Matsumoto and colleagues (Matsumoto et al., 1995). The responses seen with the concentrations of BD 1063 (1 μM) and BD 1047 (10 μM) used here are indicative of a σ-1 receptor mediated effect (Matsumoto et al., 1995). Moreover, these concentrations are identical to those used previously in our laboratory to block σ-1 receptor-mediated effects in neurons (Katnik et al., 2006; Herrera et al., 2008).

The fact that a two-site Langmuir-Hill equation was required to fit the concentration-response relationship for afobazole inhibition of microglial migration suggests that these effects may be mediated by two receptors. The interaction with a second receptor was confirmed via the use of σ-2 receptor-subtype selective antagonists. The afobazole block of microglial migration was lessened by both rimcazole and SM-21. The fact that these molecules are effective at the nanomolar range confirms that afobazole acts as an agonist at σ-2 receptors to block microglial migration (Husbands et al., 1999; Ghelardini et al., 2000).

The effects of afobazole on microglial function may in part explain the clinical benefits of afobazole. Data presented here clearly demonstrate that afobazole is an agonist for σ receptors in microglial cells. Our laboratory has shown that activation of σ receptors on microglial cells decreases the secretion of proinflammatory cytokines, and in particular, TNF-$\alpha$, by these cells (Hall et al., 2009). TNF-$\alpha$ has been linked to both anxiety and depression (Connor et al., 1998; Tuglu et al., 2003), and treatments that reduce TNF-$\alpha$ or prevent binding of this cytokine to its receptors is associated with reduction of affective disorder symptoms (Tuglu et al., 2003). Thus, afobazole, may reduce the incidence of affective disorders by reducing the production of TNF-$\alpha$ in microglia. In animals, afobazole has been shown to be effective at decreasing the incidence of learned helplessness in a rat model of depression (Uyanaev and Fisenko, 2006). Data presented here

18

demonstrate that application of afobazole can decrease the activity of P2X receptors in microglial cells.  A recent study using mice deficient in P2X7 receptors, which are primarily expressed in microglia and peripheral macrophages, showed that these mice exhibited an antidepressant-like profile (Basso et al., 2009).  Thus, by blocking P2X7 receptors, afobazole may decrease the incidence of depression.

In vivo, resting microglia exhibit a ramified morphology characterized by fine processes, or filopodia, that are highly dynamic and capable of rapidly moving towards a site of neuronal injury in response to a chemoattractant, such as ATP (Davalos et al., 2005). Prolonged activation of the microglia results in membrane ruffling, which involves withdrawal of the filopodia and conversion of the microglia into an amoeboid phenotype that is associated with an inflammatory state (Kreutzberg, 1996; Lyons et al., 2000).  Our laboratory has shown that σ receptor activation depresses the intracellular calcium signaling necessary for membrane ruffling to take place (Hall et al., 2009).   Here we show that afobazole can prevent these increases in $[Ca^{2+}]_i$ by acting on both σ-1 and σ-2 receptors.  When ATP is used as the activating molecule, metabotropic P2Y12 receptors are responsible for increases in $[Ca^{2+}]_i$ which are critical for triggering this phenomenon (Honda et al., 2001).  The fact that afobazole prevents UTP-evoked increases in $[Ca^{2+}]_i$ indicates that afobazole is blocking P2Y $[Ca^{2+}]_i$ signaling.  The activation of P2X4 receptors expressed in microglia also contributes to ATP-evoked increases in $[Ca^{2+}]_i$.  Given that afobazole also inhibits P2X channel function, $[Ca^{2+}]_i$ elevations that may be attributed to these channels will also be suppressed by afobazole.

While some studies have indicated that microglia may play a role in neurodegeneration in various CNS pathophysiological states (Streit et al., 2004), other studies have suggested that microglia may be beneficial in certain diseases.  Resting microglia have been shown to harbor BDNF and provide neuroprotection following traumatic brain injury in heat-acclimated mice (Shein et al., 2008).  Similarly, intravenous transplantation of the human microglia cell line

19

HM06 into rats after MCAO decreases infarct volume and improves behavioral recovery (Narantuya et al., 2008). Two common results of microglial responses in heat-acclimated mice and the HM06 transplantation model are: 1) a decrease in proinflammatory cytokines and 2) an increase in trophic factors in the brain (Shein et al., 2007; Narantuya et al., 2008; Shein et al., 2008). Thus, preventing the conversion of microglia into proinflammatory mediators and enhancing the survival of resting microglia is likely to provide the greatest benefit to stroke patients from a therapeutic standpoint. Data presented here indicate that afobazole can decrease microglial activation. Furthermore, afobazole functions as a cytoprotective agent and decreases microglial death caused by ischemia. When afobazole was applied to microglia during an ischemic episode, microglial cell death was significantly reduced. It was noted that cell death continued even when microglia were removed from the ischemic conditions and permitted to recover for 24 hours. Incubating the microglia in afobazole also prevented this delayed cell death caused by ischemia. Importantly, microglial cell death could be significantly reduced even if afobazole was applied after the ischemic episode. Thus, afobazole may be used to mitigate injury to microglia following an ischemic stroke, raising the possibility that afobazole can be cytoprotective at delayed time points.

In conclusion, it has been shown previously that activated microglia are involved in the inflammatory response accompanying neuronal injury during various disease states, including Alzheimer's, Parkinson's, multiple sclerosis, traumatic brain injury and stroke. However, previous studies have also concluded that resting microglia can provide trophic factors that lessen the loss of neurons in response to some, if not all, of these diseases. Here we show that afobazole acts as an agonist at both σ-1 and σ-2 receptors to prevent microglial activation, as reflected by inhibition of cell migration and decreasing $[Ca^{2+}]_i$ elevations produced by ATP and UTP. In addition, afobazole is an effective glia-protective drug that significantly reduces microglial cell death during and following an ischemic injury. Thus, afobazole is a potent modulator of microglia. The effects of afobazole on microglia may in part explain the clinical

20

benefits of this drug in affective disorders, and raises the possibility that afobazole can be a

useful therapeutic agent for the treatment of diseases involving microglia, such as ischemic

stroke.

**Acknowledgments:**

**Authorship Contributions:**

*Participated in research design*: Cuevas and Katnik.

*Conducted experiments*: Cuevas, Rodriguez, Behensky and Katnik.

*Performed data analysis*: Cuevas, Rodriguez, Behensky and Katnik.

*Wrote or contributed to the writing of the manuscript*: Cuevas and Katnik.

**References:**

Ajmo CT, Jr., Vernon DO, Collier L, Pennypacker KR and Cuevas J (2006) Sigma receptor activation reduces infarct size at 24 hours after permanent middle cerebral artery occlusion in rats. *Curr Neurovasc Res* **3**:89-98.

Basso AM, Bratcher NA, Harris RR, Jarvis MF, Decker MW and Rueter LE (2009) Behavioral profile of P2X7 receptor knockout mice in animal models of depression and anxiety: relevance for neuropsychiatric disorders. *Behav Brain Res* **198**:83-90.

Bucolo C, Drago F, Lin LR and Reddy VN (2006) Sigma receptor ligands protect human retinal cells against oxidative stress. *Neuroreport* **17**:287-291.

Connor TJ, Song C, Leonard BE, Merali Z and Anisman H (1998) An assessment of the effects of central interleukin-1beta, -2, -6, and tumor necrosis factor-alpha administration on some behavioural, neurochemical, endocrine and immune parameters in the rat. *Neuroscience* **84**:923-933.

Cuevas J and Berg DK (1998) Mammalian nicotinic receptors with alpha7 subunits that slowly desensitize and rapidly recover from alpha-bungarotoxin blockade. *J Neurosci* **18**:10335-10344.

Davalos D, Grutzendler J, Yang G, Kim JV, Zuo Y, Jung S, Littman DR, Dustin ML and Gan WB (2005) ATP mediates rapid microglial response to local brain injury in vivo. *Nat Neurosci* **8**:752-758.

Dheen ST, Kaur C and Ling EA (2007) Microglial activation and its implications in the brain diseases. *Curr Med Chem* **14**:1189-1197.

Galaeva IP, Garibova TL, Voronina TA and Seredenin SB (2005) Neuroprotective effects of afobazol in experimental cerebral hemorrhage. *Bull Exp Biol Med* **140**:535-537.

Ghelardini C, Galeotti N and Bartolini A (2000) Pharmacological identification of SM-21, the novel sigma(2) antagonist. *Pharmacol Biochem Behav* **67**:659-662.

Hall AA, Herrera Y, Ajmo CT, Jr., Cuevas J and Pennypacker KR (2009) Sigma receptors suppress multiple aspects of microglial activation. *Glia* **57**:744-754.

Hanisch UK and Kettenmann H (2007) Microglia: active sensor and versatile effector cells in the normal and pathologic brain. *Nat Neurosci* **10**:1387-1394.

Herrera Y, Katnik C, Rodriguez JD, Hall AA, Willing A, Pennypacker KR and Cuevas J (2008) sigma-1 receptor modulation of acid-sensing ion channel a (ASIC1a) and ASIC1a-induced Ca2+ influx in rat cortical neurons. *J Pharmacol Exp Ther* **327**:491-502.

Honda S, Sasaki Y, Ohsawa K, Imai Y, Nakamura Y, Inoue K and Kohsaka S (2001) Extracellular ATP or ADP induce chemotaxis of cultured microglia through Gi/o-coupled P2Y receptors. *J Neurosci* **21**:1975-1982.

Husbands SM, Izenwasser S, Kopajtic T, Bowen WD, Vilner BJ, Katz JL and Newman AH (1999) Structure-activity relationships at the monoamine transporters and sigma receptors for a novel series of 9-[3-(cis-3, 5-dimethyl-1-piperazinyl)propyl]carbazole (rimcazole) analogues. *J Med Chem* **42**:4446-4455.

Katnik C, Guerrero WR, Pennypacker KR, Herrera Y and Cuevas J (2006) Sigma-1 receptor activation prevents intracellular calcium dysregulation in cortical neurons during in vitro ischemia. *J Pharmacol Exp Ther* **319**:1355-1365.

Kitamura Y, Takata K, Inden M, Tsuchiya D, Yanagisawa D, Nakata J and Taniguchi T (2004) Intracerebroventricular injection of microglia protects against focal brain ischemia. *J Pharmacol Sci* **94**:203-206.

Kreutzberg GW (1996) Microglia: a sensor for pathological events in the CNS. *Trends Neurosci* **19**:312-318.

Lalancette-Hebert M, Gowing G, Simard A, Weng YC and Kriz J (2007) Selective ablation of proliferating microglial cells exacerbates ischemic injury in the brain. *J Neurosci* **27**:2596-2605.

Lyons SA and Kettenmann H (1998) Oligodendrocytes and microglia are selectively vulnerable to combined hypoxia and hypoglycemia injury in vitro. *J Cereb Blood Flow Metab* **18**:521-530.

Lyons SA, Pastor A, Ohlemeyer C, Kann O, Wiegand F, Prass K, Knapp F, Kettenmann H and Dirnagl U (2000) Distinct physiologic properties of microglia and blood-borne cells in rat brain slices after permanent middle cerebral artery occlusion. *J Cereb Blood Flow Metab* **20**:1537-1549.

Matsumoto RR, Bowen WD, Tom MA, Vo VN, Truong DD and De Costa BR (1995) Characterization of two novel sigma receptor ligands: antidystonic effects in rats suggest sigma receptor antagonism. *Eur J Pharmacol* **280**:301-310.

Narantuya D, Nagai A, Sheikh AM, Masuda J, Kobayashi S, Yamaguchi S and Kim SU (2008) Human microglia transplanted in rat focal ischemia brain induce neuroprotection and behavioral improvement. *PLoS One* **5**:e11746.

Rae J, Cooper K, Gates P and Watsky M (1991) Low access resistance perforated patch recordings using amphotericin B. *J Neurosci Methods* **37**:15-26.

Rogove AD, Lu W and Tsirka SE (2002) Microglial activation and recruitment, but not proliferation, suffice to mediate neurodegeneration. *Cell Death Differ* **9**:801-806.

Seredenin SB, Antipova TA, Voronin MV, Kurchashova SY and Kuimov AN (2009) Interaction of afobazole with sigma1-receptors. *Bull Exp Biol Med* **148**:42-44.

Seredenin SB, Romanova GA and Shakova FM (2008) Neuroprotective effect of afobazole on rats with bilateral local photothrombosis of vessels in the prefrontal cortex. *Bull Exp Biol Med* **145**:207-209.

Shein NA, Doron H, Horowitz M, Trembovler V, Alexandrovich AG and Shohami E (2007) Altered cytokine expression and sustained hypothermia following traumatic brain injury in heat acclimated mice. *Brain Res* **1185**:313-320.

Shein NA, Grigoriadis N, Horowitz M, Umschwief G, Alexandrovich AG, Simeonidou C, Grigoriadis S, Touloumi O and Shohami E (2008) Microglial involvement in neuroprotection following experimental traumatic brain injury in heat-acclimated mice. *Brain Res* **1244**:132-141.

Streit WJ, Mrak RE and Griffin WS (2004) Microglia and neuroinflammation: a pathological perspective. *J Neuroinflammation* **1**:14.

Tuglu C, Kara SH, Caliyurt O, Vardar E and Abay E (2003) Increased serum tumor necrosis factor-alpha levels and treatment response in major depressive disorder. *Psychopharmacology (Berl)* **170**:429-433.

Uyanaev AA and Fisenko VP (2006) Studies of long-term noopept and afobazol treatment in rats with learned helplessness neurosis. *Bull Exp Biol Med* **142**:202-204.

Weinstein JR, Koerner IP and Moller T (2010) Microglia in ischemic brain injury. *Future Neurol* **5**:227-246.

Wu Z, Gebreselassie, D., Williams, W., Bowen, W.D. (2003) Reexamination of metaphit as a tool for the study of sigma receptors, in *Society for Neuroscience*, Washington, DC.

Zenina TA, Gavrish IV, Melkumyan DS, Seredenina TS and Seredenin SB (2005) Neuroprotective properties of afobazol in vitro. *Bull Exp Biol Med* **140**:194-196.

Zhang H and Cuevas J (2002) Sigma receptors inhibit high-voltage-activated calcium channels in rat sympathetic and parasympathetic neurons. *J Neurophysiol* **87**:2867-2879.

**Footnotes:**

**Legends for Figures:**

Figure 1: Afobazole blocks the migration of microglia elicited by ATP and UTP.  A,

Photomicrographs of microglia that migrated in response to 100 $\mu$M ATP (left panels) or 100 $\mu$M

UTP (right panels) in the absence (Control) or presence of afobazole at the indicated

concentrations.  Microglia nuclei were labeled with DAPI and appear as white dots.  Fields of

view are 0.221 mm$^2$, and scale bar in bottom left panel (ATP, 300 $\mu$M afobazole) is 50 $\mu$m.  B,

Concentration-response relationship for afobazole inhibition of microglial migration evoked by

100 $\mu$M ATP (closed circles) or 100 $\mu$M UTP (open circles).  Solid line represents best fit to the

ATP data using a two-component Langmuir-Hill equation with the $E_{max}$, $IC_{50}$ and Hill coefficient

being 0.46, 1.4 $\mu$M and 0.46 for the high affinity component and 0.55, 117 $\mu$M and 1.4  for the low

affinity component, respectively.  Dashed line represents best fit to the UTP data using a two-

component Langmuir-Hill equation with the $E_{max}$, $IC_{50}$ and Hill coefficient being 0.51, 3.0 $\mu$M, and

0.64 for the high affinity component and 0.49, 102 $\mu$M, and 2.1 for the low affinity component,

respectively.  Points represent mean ($\pm$SEM) and for all points, n > 6.

Figure 2: The pan-selective sigma receptor antagonist, metaphit, depresses afobazole inhibition of

ATP- and UTP-evoked elevations of $[Ca^{2+}]_i$ in microglial cells. A, Mean number ($\pm$SEM) of

microglial cells migrating in response to application of 100 $\mu$M ATP in the absence and presence of

30 $\mu$M afobazole (Afobazole) or 100 $\mu$M DTG (DTG) when the cells were preincubated in normal

media (Media) or media containing metaphit (Metaphit; 50 $\mu$M, 15 min, room temperature).

Asterisks denote significant difference from Control group within Media (p < 0.001) and Metaphit (p

< 0.001), respectively, and pound symbol denotes significant difference within Control between

Media and Metaphit (p < 0.001).   B, Mean percent inhibition of ATP-induced migration produced

by 30 $\mu$M afobazole and 30 $\mu$M DTG when the cells were preincubated in normal media (Media) or

media containing metaphit (Metaphit).  Asterisks denote significant difference between Media and

Metaphit groups within Afobazole and DTG, respectively (p < 0.001 for both).  C, Identical

experiments as panel (A) using 100 μM UTP as the chemoattractant.  Asterisks denote significant

difference from Control group within Media (p < 0.001) and Metaphit (p < 0.001), respectively, and

pound symbols denote significant difference between Media and Metaphit within each respective

group (p < 0.001 for all).  Daggers indicate significant difference between afobazole and DTG

within Media and Metaphit groups, respectively.  D,   Mean percent inhibition of UTP-evoked

migration produced by 30 μM afobazole and 30 μM DTG when the cells were preincubated in

normal media (Media) or media containing metaphit (Metaphit).  Asterisks denote significant

difference between Media and Metaphit groups within Afobazole and DTG, respectively (p < 0.001

for both).  For panels (A) and (B) n = 18 in all groups and for panels (C) and (D) n = 6 for all

groups.

Figure 3: Inhibition of σ-1 receptors blocks afobazole-mediated disruption of microglial

migration.  A, Bar graph of the mean (± SEM) number of microglial cells migrating in response to

100 μM ATP when ATP was added alone (ATP); when ATP was added in the presence of 30 μM

afobazole (Afob), 1 μM BD-1063 (BD-1063), 10 μM BD-1047 (BD-1047) or 100 μM NE-100 (NE-

100); and when ATP was added with afobazole in the presence of the respective antagonists at

these concentrations.  Pound symbols denote significant difference between afobazole groups and

their respective controls (i.e. BD-1063 and BD-1063 + Afob).  Asterisks indicate significant

difference from ATP control (ATP) or afobazole control (Afob) (p < 0.001), and n = 6 for all groups.

B, Percent inhibition of microglial migration in response to 100 μM ATP evoked by 30 μM afobazole

in the absence (Control) and presence of the indicated σ-1 antagonists at the same concentrations

as in panel (A).  Asterisks denote significant difference from Control group (p < 0.001), and n = 6

for all conditions. Field of view is 0.221 mm$^2$ in (A) and (C).

Figure 4: Afobazole-mediated inhibition of microglial migration is blocked by σ-2 receptor

antagonists. A, Bar graph of the mean number of microglial cells migrating in response to 100 μM

ATP when ATP was added alone (ATP); when ATP was added in the presence of 30 μM

afobazole (Afob), 10 nM rimcazole (Rim) or 1 nM SM21 (SM21); and when ATP was added with

afobazole in the presence of the respective antagonists at these concentrations.  Pound symbols

denote significant difference between afobazole groups and their respective controls (i.e. Rim and

Rim + Afob).  Asterisks indicate significant difference from ATP control (ATP) or afobazole control

(Afob) (p < 0.001 for all). B, Percent inhibition of microglial migration in response to 100 μM ATP

evoked by 30 μM afobazole in the absence (Control) and presence of the indicated sigma-2

antagonists at the same concentrations as in panel (A).  Asterisks denote significant difference

from Control group (p < 0.001). For all groups, n = 6. Field of view is 0.221 mm$^2$ in (A) and (C).

Figure 5: Afobazole inhibits ATP-evoked increases in $[Ca^{2+}]_i$ in microglial cells.  A,

Representative traces of $[Ca^{2+}]_i$ as a function of time recorded from a microglial cell during

application of ATP in the absence (Control) and presence of 100 μM afobazole (Afobazole,

upper traces) or 100 μM DTG (DTG, lower traces). B, Bar graphs of mean (±SEM) increases in

peak $[Ca^{2+}]_i$ ($\Delta[Ca^{2+}]_i$) (Peak) or net $\Delta[Ca^{2+}]_i$ (Area, area under the trace) elicited by focal

application of 100 μM ATP in the absence (Control) and presence of 100 μM afobazole (n =

124) or 100 μM DTG (n = 128).  Asterisks denote significant difference from Control (p < 0.001)

and pound symbol indicates significant difference between the afobazole and DTG groups (p

<0.001).  C, Bar graph of mean percent inhibition of peak ATP-evoked increases in $[Ca^{2+}]_i$

produced by afobazole and DTG. Asterisk denotes significant difference (p <0.001).

Figure 6: Afobazole inhibits ATP-evoked membrane currents in microglial cells.  A, Traces of ATP-evoked (300 μM) membrane currents as a function of time recorded from an isolated microglial cell in the absence (Control) and presence of 300 μM afobazole (Afobazole). Cell was held at -70 mV.  B, Mean peak ATP-evoked inward current recorded from 8 microglial cells using identical methods as in (A).  Asterisk denotes significant difference ($p < 0.03$).

Figure 7: Inhibition of σ receptors with metaphit blocks afobazole-mediated depression of ATP- and UTP-evoked $[Ca^{2+}]_i$ increases.  A, Representative traces of $[Ca^{2+}]_i$ as a function of time recorded from 2 different microglial cells in response to 100 μM ATP in the absence (Control) and presence of 100 μM afobazole, without (PSS, left traces) and with 15 min preincubation in 50 μM metaphit (Metaphit, right traces). B, Bar graphs of mean (±SEM) increases in peak $[Ca^{2+}]_i$ ($\Delta[Ca^{2+}]_i$) elicited by 100 μM ATP in the absence (Control) and presence of afobazole when cells were preincubated in normal PSS (PSS, n = 37) or PSS containing 50 μM metaphit for 15 min (Metaphit, n = 36).  Asterisks denote significant differences from Control ($p < 0.05$) within the PSS and metaphit groups, respectively, and pound symbol indicates significant difference between the PSS and metaphit groups within afobazole ($p < 0.05$).  C, Bar graph of percent inhibition of ATP-evoked peak increases in $[Ca^{2+}]_i$ produced when cells were treated with 100 μM afobazole (PSS, n = 37) or with afobazole after preincubation in metaphit (Metaphit, n = 36). Asterisk denotes significant difference ($p < 0.001$). D, Representative traces of UTP-evoked $[Ca^{2+}]_i$ changes recorded from 2 different microglial cells in absence (Control) and presence of 100 μM afobazole, without (PSS, left traces) and with 15 min preincubation in 50 μM metaphit (Metaphit, right traces). E, Identical experiment as (B) using UTP as the agonist.  Asterisks denote significant differences from Control ($p < 0.05$) within the PSS (n = 90) and metaphit (n = 44) groups, respectively, and pound symbol indicates significant difference between the PSS

and metaphit groups within control and afobazole ($p < 0.05$).  F, Bar graph of percent inhibition of UTP-evoked peak increases in $[Ca^{2+}]_i$ produced when cells were treated with 100 $\mu$M afobazole (PSS, n = 90) or with afobazole after preincubation in metaphit (Metaphit, n = 44). Asterisk denotes significant difference ($p < 0.001$).

Figure 8: Inhibition of $\sigma$-1 receptors with the selective antagonists, BD 1063 and BD 1047, reduces afobazole-mediated block of ATP-evoked increases in $[Ca^{2+}]_i$. Bar graphs of mean ($\pm$SEM) increases in peak $[Ca^{2+}]_i$ ($\Delta[Ca^{2+}]_i$) elicited by 100 $\mu$M ATP in the absence (Control) and presence of afobazole (Afobazole) when cells were treated in normal PSS (PSS) or PSS containing 100 $\mu$M BD 1063 (A) or 10 $\mu$M BD 1047 (B).  Cells were incubated with antagonists for 5 minutes before being incubated with afobazole.  Asterisks denote significant differences from Control ($p < 0.001$) within the PSS and $\sigma$-1 antagonist groups, respectively, and pound symbols indicate significant difference between the PSS and $\sigma$-1 antagonist groups within afobazole ($p < 0.001$).  Bar graphs of percent inhibition of ATP-evoked peak increases in $[Ca^{2+}]_i$ produced when cells were treated with 100 $\mu$M afobazole (PSS) or with afobazole and the $\sigma$-1 antagonists BD 1063 (C) or BD 1047 (D).  Asterisks denote significant difference ($p < 0.001$). For (A and C): PSS, n = 220; BD 1063, n = 150. For (B and D): PSS, n = 300; BD 1047, n = 249.

Figure 9: Inhibition of $\sigma$-2 receptors with the selective antagonists, SM 21 and rimcazole, reduces afobazole-mediated block of ATP-evoked increases in $[Ca^{2+}]_i$. Bar graphs of mean ($\pm$SEM) increases in peak $[Ca^{2+}]_i$ ($\Delta[Ca^{2+}]_i$) elicited by 100 $\mu$M ATP in the absence (Control) and presence of afobazole (Afobazole) when cells were treated in normal PSS (PSS) or PSS containing 10 $\mu$M SM 21 (A) or 10 $\mu$M rimcazole (B).  Asterisks denote significant differences from Control ($p < 0.001$) within the PSS and $\sigma$-2 antagonist groups, respectively, and pound

symbols indicate significant difference between the PSS and σ-2 antagonist groups within afobazole (SM 21, p < 0.03; rimcazole, p <0.001) and control (p < 0.03, rimcazole only). Bar graphs of percent inhibition of ATP-evoked peak increases in $[Ca^{2+}]_i$ produced when cells were treated with 100 μM afobazole (PSS) or with afobazole and the σ-1 antagonists SM 21 (C) or rimcazole (D). Asterisks denote significant difference (p < 0.001). For (A and C): PSS, n = 202; SM 21, n = 194. For (B and D): PSS, n = 141; rimcazole, n = 152.

Figure 10: Effects of afobazole and DTG on microglial cell survival in response to in vitro ischemia. Bar graphs of mean (± SEM) cell death measured in microglial cells cultures using lactate dehydrogenase (LDH) cytotoxicity assays. Values were normalized to LDH levels measured in the DMEM group in the absence of ischemia (DMEM, Control). All control groups were maintained at 37° C and under normoxic conditions. Ischemia groups were incubated in glucose-free medium containing 4 mM sodium azide and under hypoxic conditions (at 37° C) for 2 hrs. LDH was measured in the medium after this 2-hr period (A) or after a 24 hr recovery period (B). Total LDH (2 hr + 24 hr) is shown in panel (C). Asterisks denote significant differences from DMEM group within Control and Ischemia (p < 0.001), pound symbols indicate significant difference between afobazole and DTG at 30 μM and 100 μM (p < 0.001). Daggers denote difference between 30 μM and 100 μM concentrations for each drug (p < 0.001). Percent inhibition of ischemia-induced cell death produced by afobazole and DTG at 30 μM (Afob 30, DTG 30) and 100 μM (Afob 100, DTG 100) concentrations, respectively. Percent inhibition was determined immediately after the 2 hr ischemic insult (D) and after a 24 hr recovery (E). Percent inhibition of total ischemia-induced cell death is shown in panel (F). Ischemia-induced cell death was determined by subtracting the mean LDH value obtained for each control group from their respective ischemia group. These values were then used to calculate percent inhibition of cell death relative to the ischemia DMEM group. Pound symbols in (D) and (F) indicate difference between 30 μM and 100 μM concentrations of

35

each drug ($p < 0.05$). Asterisks in (F) denote significant difference between 30 $\mu$M and 100 $\mu$M afobazole and equivalent DTG concentrations ($p < 0.05$). For all groups, n > 9.

Figure 11: Time-dependence of the effects of afobazole on microglial cell death caused by ischemia. Bar graphs of mean (± SEM) cell death measured by lactate dehydrogenase (LDH) cytotoxicity assays in cultured microglial cells. Values were normalized to LDH levels measured in the DMEM group in the absence of ischemia (DMEM, Control). All control groups were maintained at 37° C and under normoxic conditions. Ischemia groups were incubated in glucose-free medium containing 4 mM sodium azide and under hypoxic conditions (at 37° C) for 2 hrs. LDH was measured in the medium after this 2-hr period (A) or after a 24 hr recovery period (B). Total LDH (2 hr + 24 hr) is shown in panel (C). Groups were treated with either DMEM throughout (DMEM) or DMEM during the 2 hr ischemic episode followed by 30 $\mu$M (DMEM-Afob 30) or 100 $\mu$M (DMEM-Afob 100) afobazole during the 24 hr recovery. Asterisks denote significant differences between afobazole treatment groups and groups treated with DMEM within Ischemia ($p < 0.001$). Note that during the 2hr ischemia all groups were treated only with DMEM for these studies. Percent inhibition of ischemia-induced cell death observed when cells were treated with DMEM during the ischemic episode followed by afobazole at 30 $\mu$M (DMEM-Afob 30) and 100 $\mu$M (DMEM-Afob 100) concentrations during the 24 hr recovery period. Percent inhibition was determined immediately after the 2 hr ischemic insult (D) and after the 24 hr recovery (E). Percent inhibition of total ischemia-induced cell death is shown in panel (F). For all groups, n = 6.
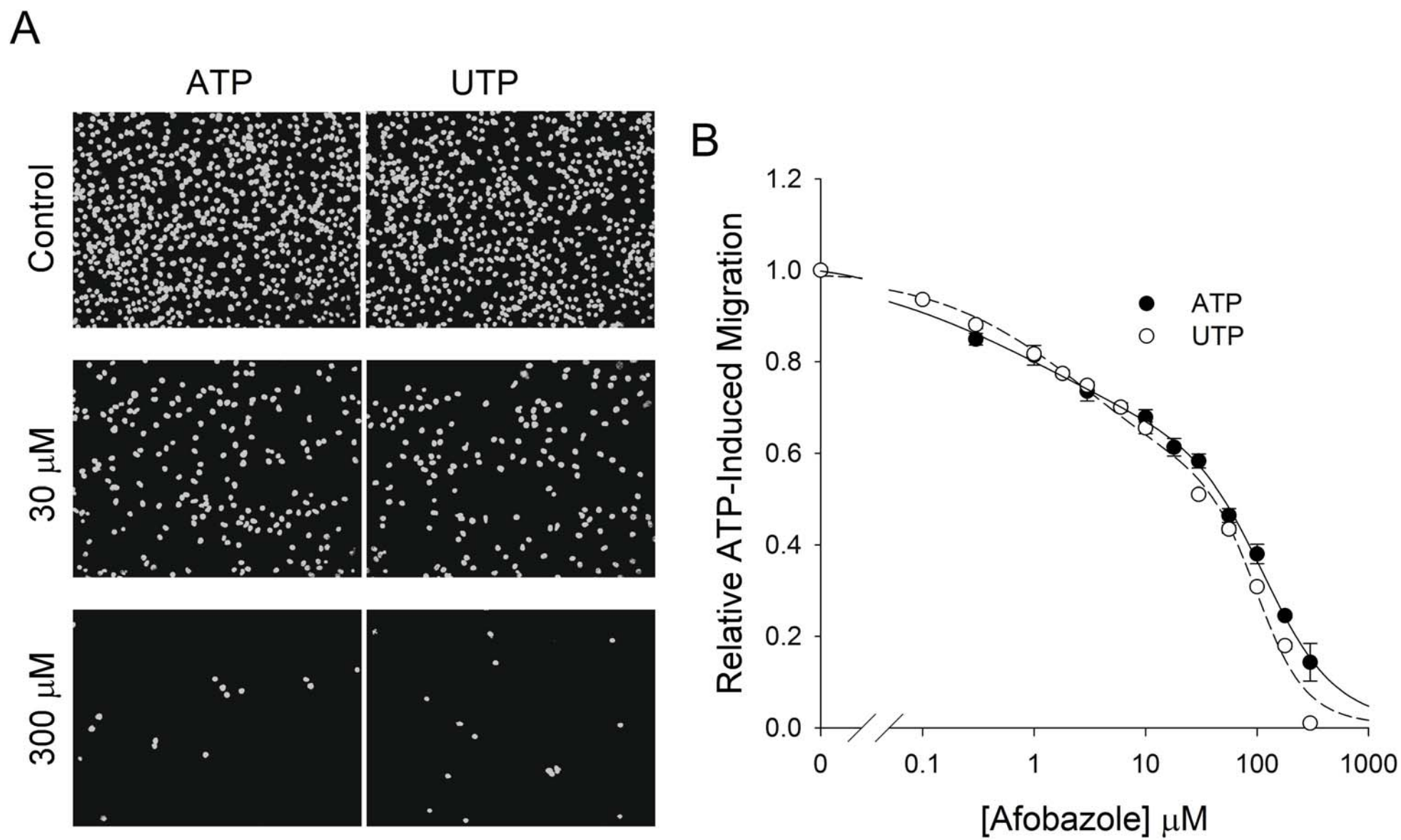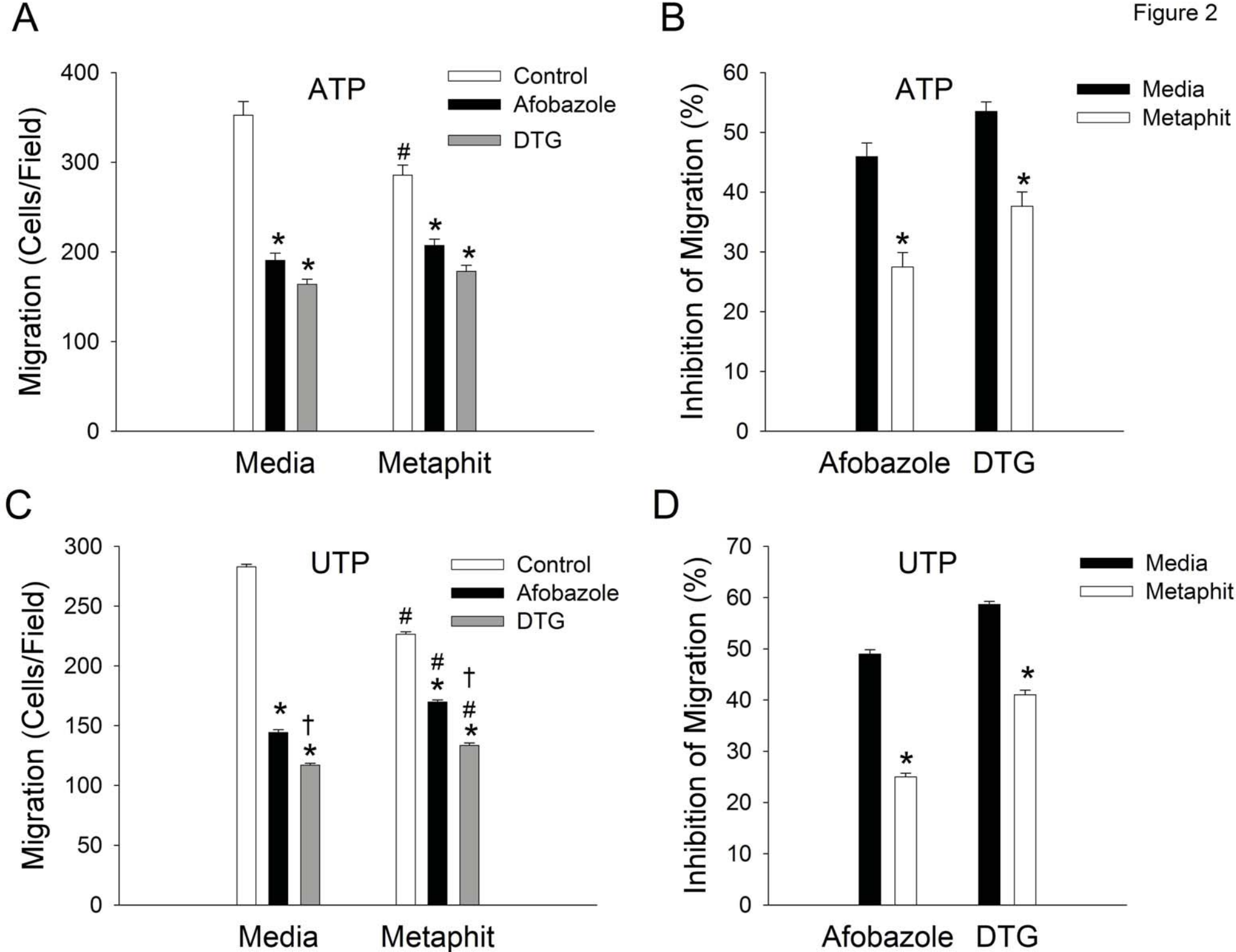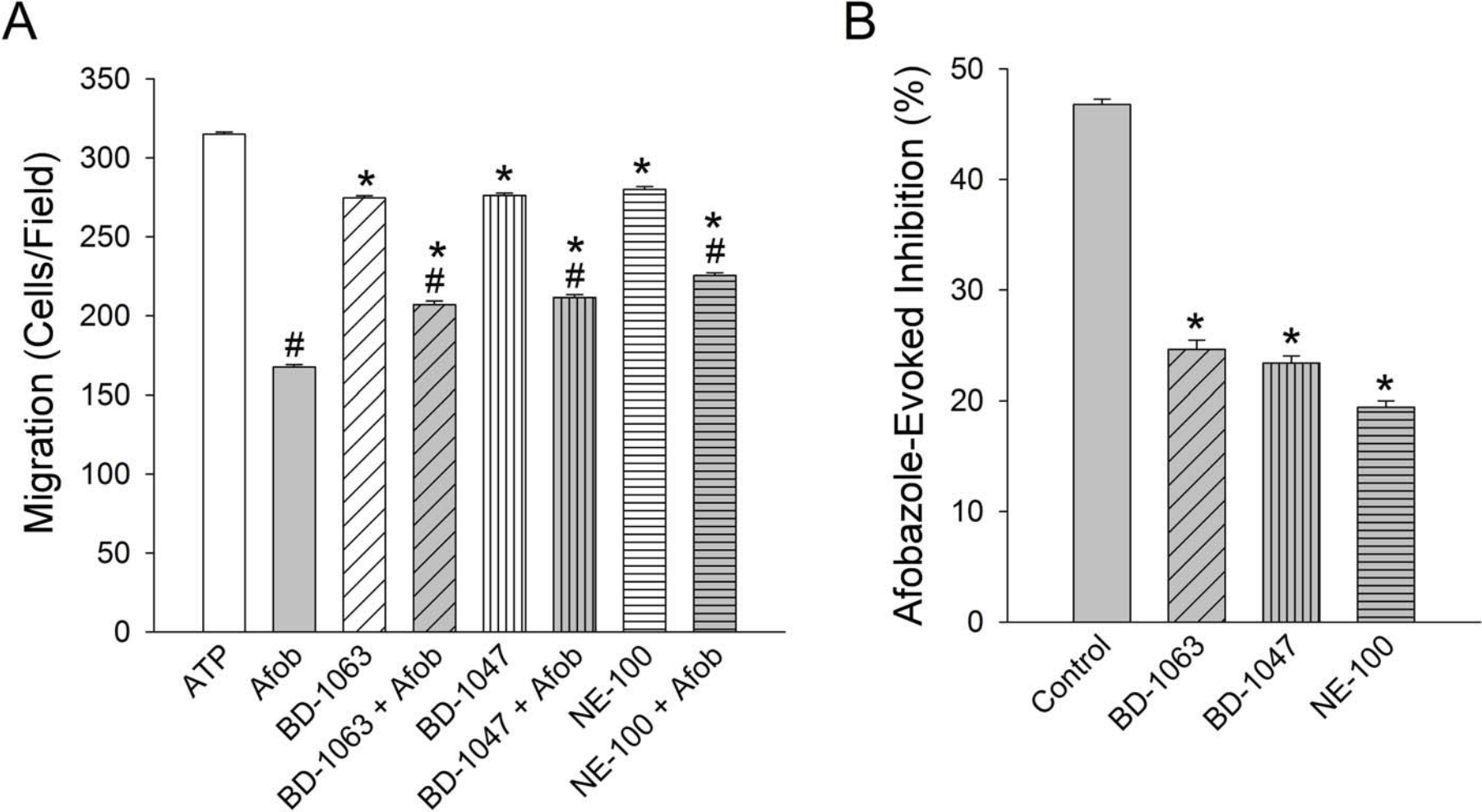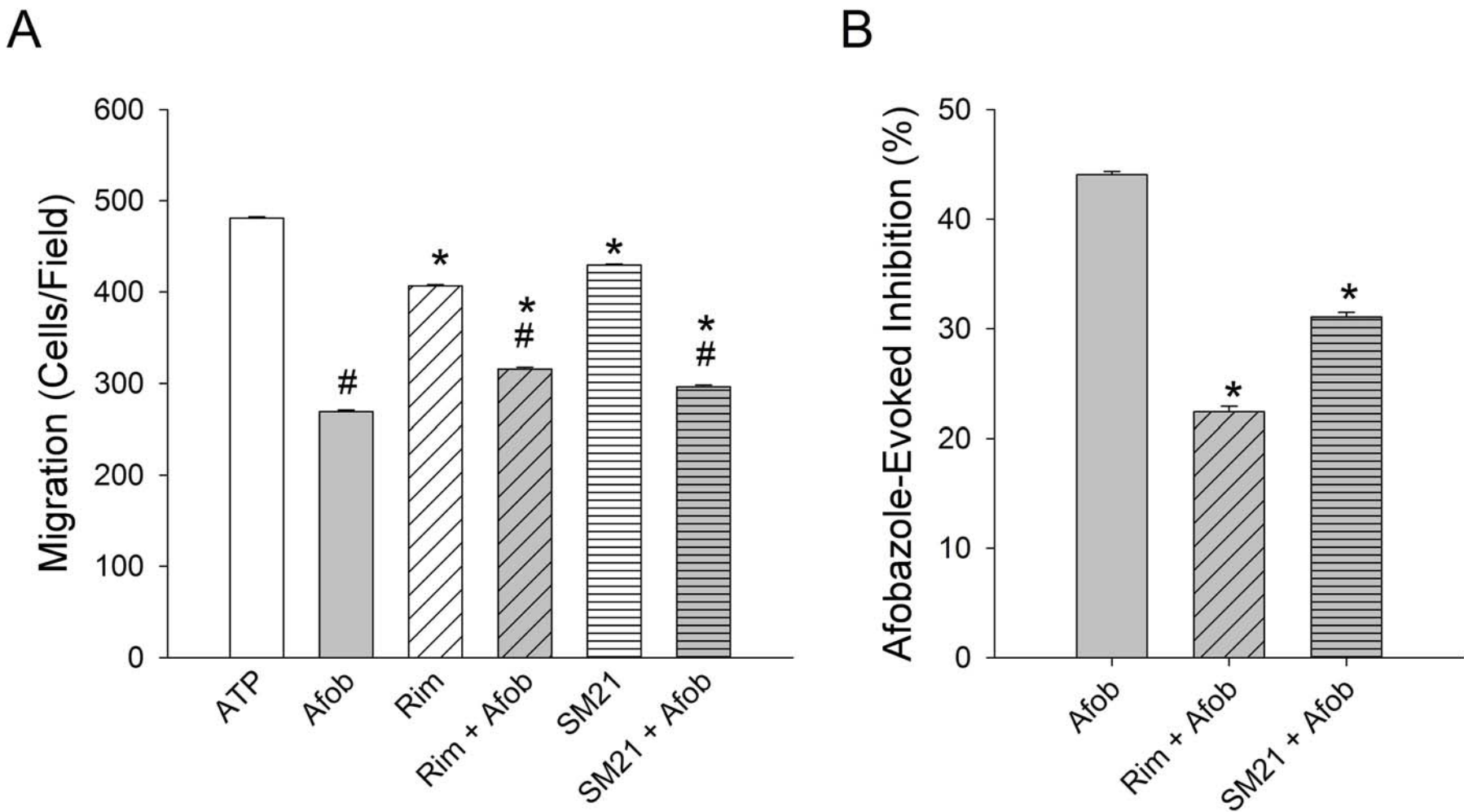
Figure 1

A



B

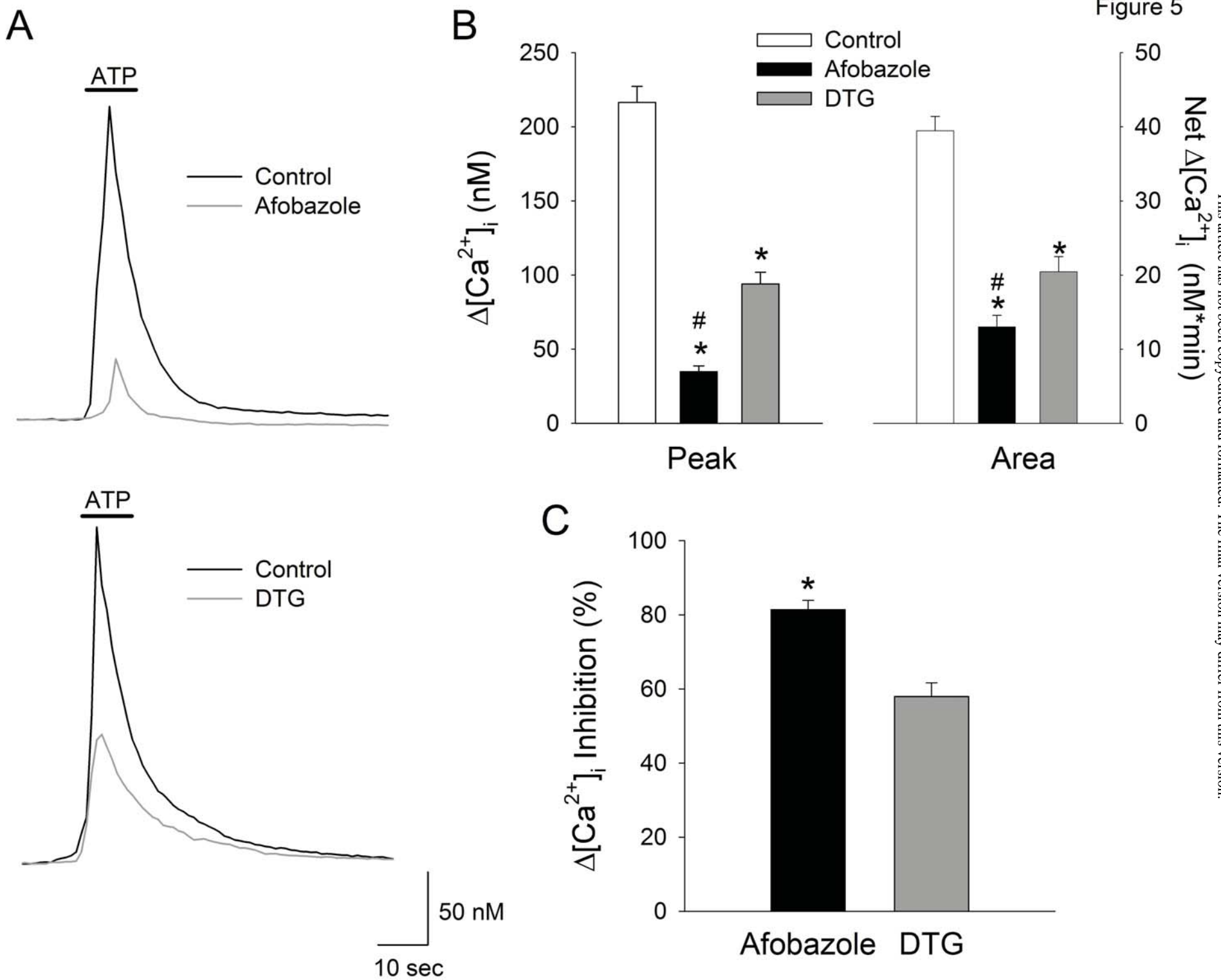Figure 2

Figure 3

Figure 4

Figure 5

Figure 6



A  Control
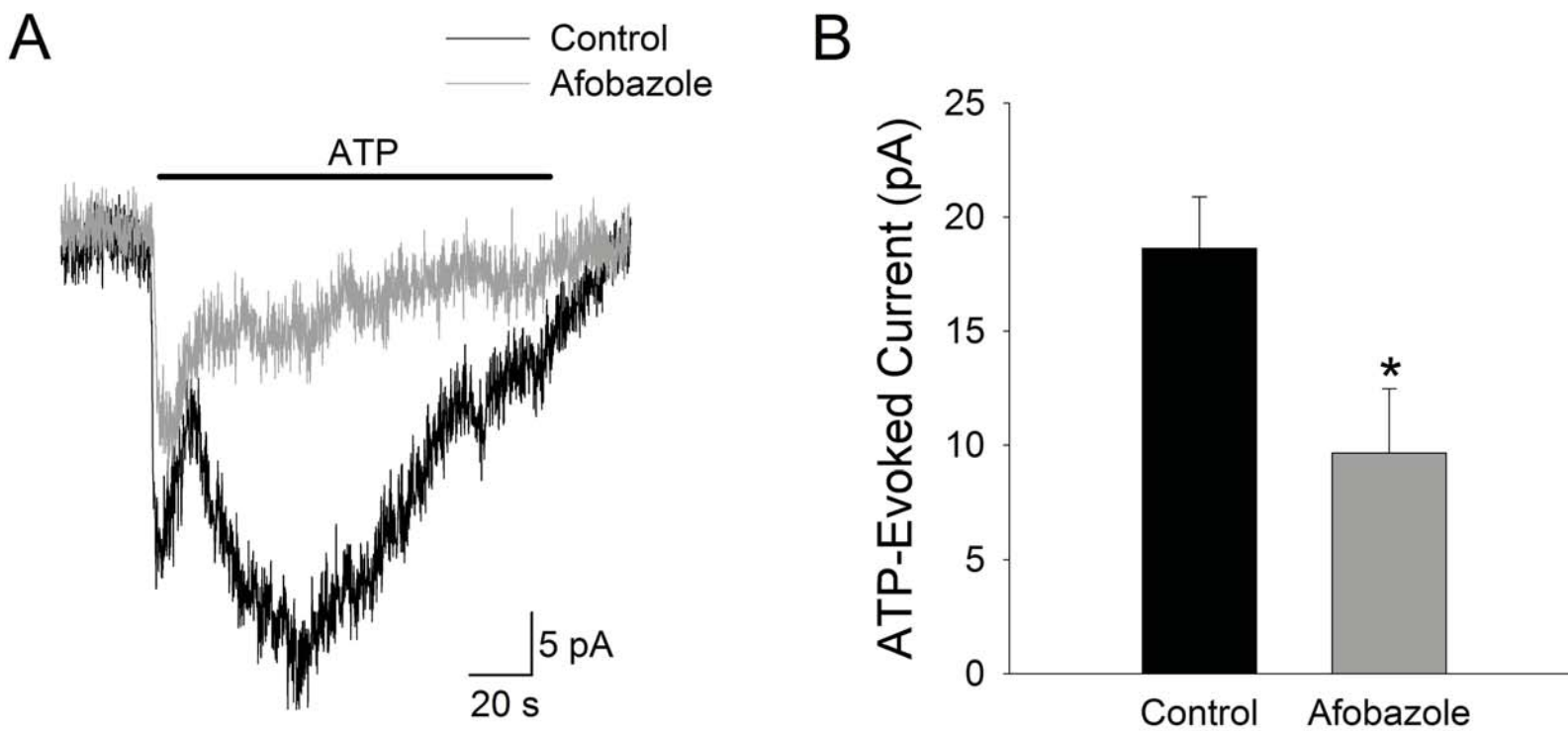   Afobazole

ATP

5 pA
20 s
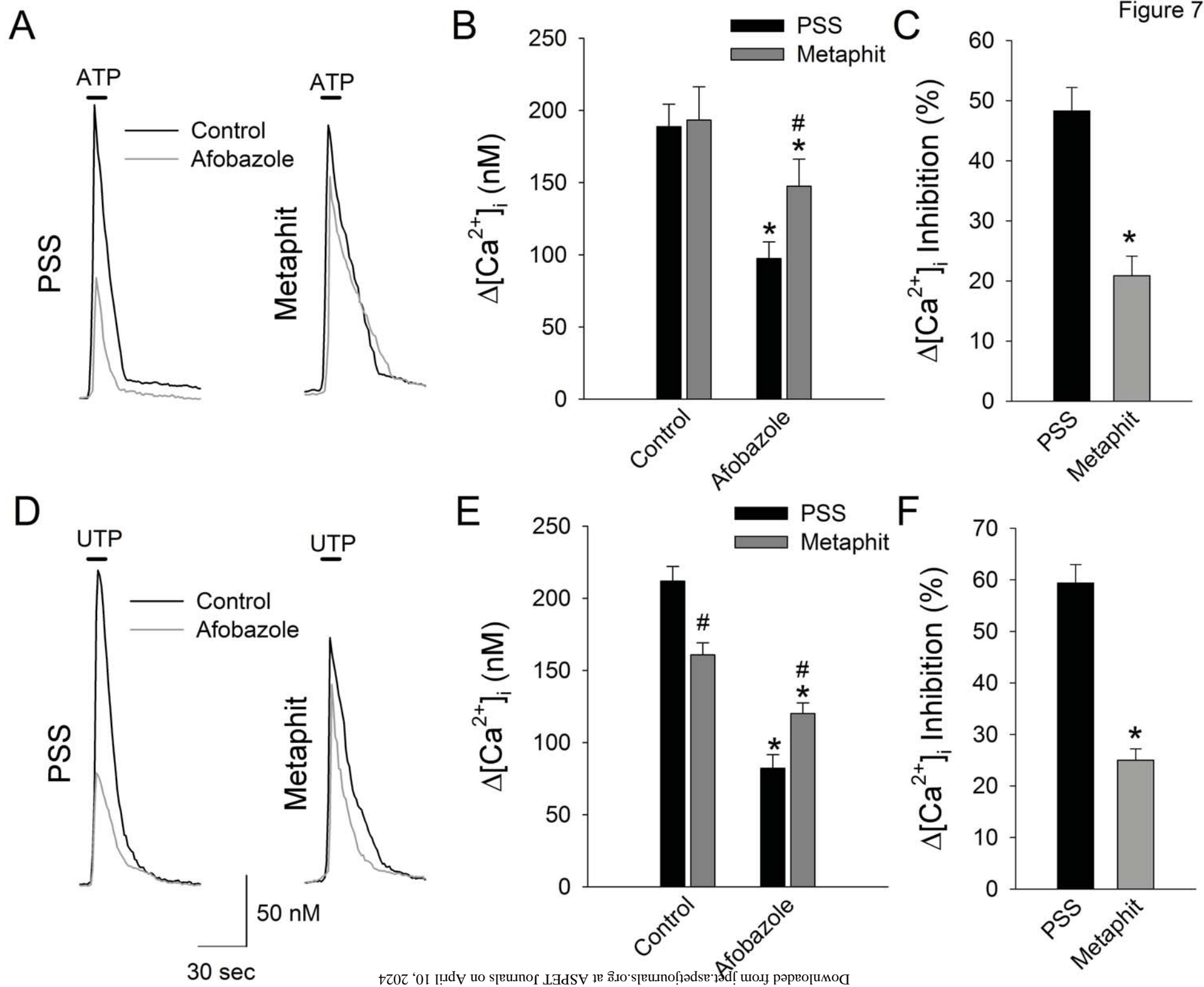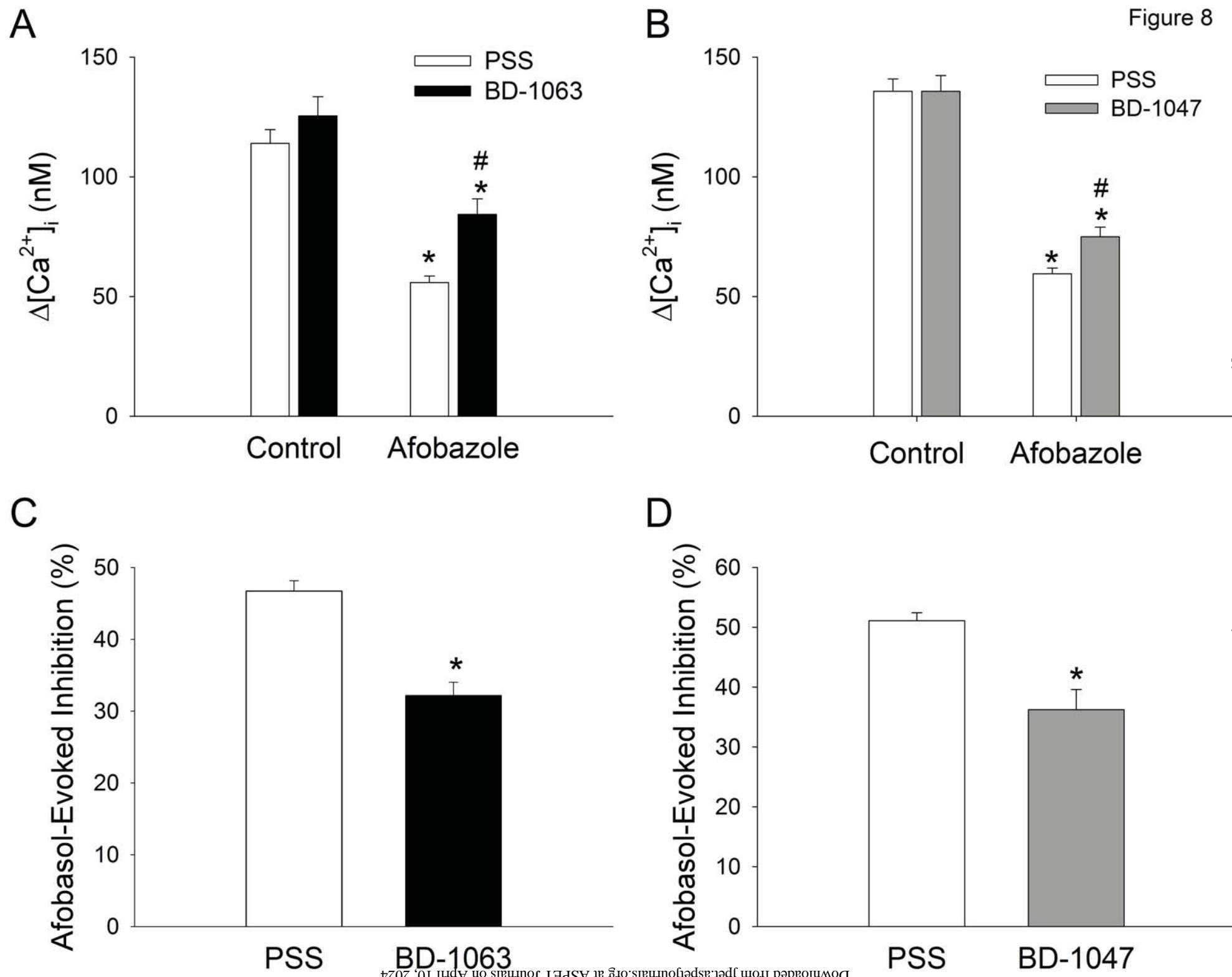
B

ATP-Evoked Current (pA)

25
20
15
10
5
0

Control   Afobazole

*

Figure 7

Figure 8

Figure 9

Figure 10

Figure 11